Available online at www.sciencedirect.com
SCIENCE DIRECT®
C. R. Physique 5 (2004) 249–258
COMPTES RENDUS PHYSIQUE

Gas phase molecular spectroscopy/Spectroscopie moléculaire en phase gazeuse

Optical diagnostic of temperature in rocket engines by coherent Raman techniques

Frédéric Chaussard [a,*], Xavier Michaut [a], Robert Saint-Loup [a], Hubert Berger [a], Paul Bouchardy [b], Frédéric Grisch [b]

[a] *Laboratoire de physique, UMR CNRS 5027, Université de Bourgogne, BP 47870, 21078 Dijon cedex, France*
[b] *Office national d'études et de recherches aérospatiales, département mesures physiques, Fort de Palaiseau, 91761 Palaiseau cedex, France*

Presented by Guy Laval

Abstract

This article reviews the study of Raman line shapes of molecular species involved in reactive media, such flames or engines, at high temperature and high pressure. This study is of interest from a fundamental as well as from a practical point of view with regards to the CARS temperature diagnostic of GH_2–LOX combustion systems. We will particularly draw attention to recent investigations by means of Stimulated Raman Spectroscopy (SRS) in H_2–H_2O mixtures at temperature up to 1800 K. Whereas H_2–X systems usually exhibit large inhomogeneous effects, due to the speed dependence of the collisional parameters, the absence of such apparent inhomogeneous signatures in the H_2–H_2O system allowed us to model the broadening coefficients with simple polynomial laws. These laws permit extrapolations with a narrow confidence interval, as required for temperature measurements. The applications of these results to the temperature diagnostic on the small-scale facility MASCOTTE at ONERA will be described. ***To cite this article: F. Chaussard et al., C. R. Physique 5 (2004).***

Résumé

Diagnostic optique de la température dans des moteurs-fusée à l'aide de techniques Raman cohérentes. Nous présentons ici un résumé de l'étude de profils spectraux Raman d'espèces moléculaires présentes dans les milieux réactifs, tels les flammes ou les moteurs, à haute pression et haute température. L'intérêt de cette étude réside aussi bien dans son aspect fondamental qu'applicatif pour le diagnostic DRASC de la température dans les systèmes GH_2–LOX en combustion. Nous détaillerons tout particulièrement les mesures récentes réalisées par Spectroscopie Raman Stimulé sur les mélanges H_2–H_2O à des températures allant jusqu'à 1800 K. Alors que les systèmes H_2–X présentent généralement de forts effets inhomogènes dus à la dépendance en vitesse des paramètres collisionnels, l'absence de telles signatures inhomogènes dans le système H_2–H_2O nous a permis de modéliser les coefficients d'élargissement à l'aide de lois polynomiales simples. Ces lois permettent des extrapolations avec des intervalles de confiance étroits, comme requis pour les mesures de température. Les applications de ces résultats au diagnostic de la température sur le banc d'essai MASCOTTE de l'ONERA seront présentées. ***Pour citer cet article : F. Chaussard et al., C. R. Physique 5 (2004).***

Keywords: Collision; Combustion; Diagnostic; Line shape; Raman spectroscopy

Mots-clés : Collision ; Combustion ; Diagnostic ; Profils spectraux ; Spectroscopie Raman

* Corresponding author.
E-mail address: Frederic.Chaussard@u-bourgogne.fr (F. Chaussard).

1631-0705/$ – see front matter
doi:10.1016/j.crhy.2004.01.015

1. Introduction

The low cost development of liquid rocket engines, which must have a higher performance and be more and more reliable, is still a big challenge for manufacturers. The improvement of these engine performances depends on how the various physical and chemical mechanisms which occur in combustion are understood. However, combustion in engines fed with both liquid oxygen (LOX) and hydrogen (GH_2) at high pressure (up to 30 MPa) is so complex that modeling and simulation cannot be carried out without extensive validation based on detailed investigation of elementary processes (liquid propellant injection, atomization, droplet vaporization, turbulent mixing, combustion,...) in well defined configurations which are, nevertheless, representative operating conditions.

In this context, a cooperative research program on combustion in liquid rocket engines has been conducted in Germany and France in the framework of a joint venture between industry (SNECMA Moteurs-fusées, Astrium), the French space agency (CNES) and research organizations (ONERA and CNRS) so as to generate a fundamental understanding of the combustion mechanisms, and to develop an experimental database required for computer modeling. These experiments were run on the cryogenic test facility called MASCOTTE developed by Onera. Obtaining reliable data from cryogenic combustion in such conditions still represents a big challenge due to the experimental constraints imposed by the hostile environment and the severe running conditions: the pressure in the combustion chamber is about 12 Mpa and the temperature can reach 3000 K. Optical techniques with their high spatial and temporal resolution offer the greatest potential for these studies. Several optical techniques have been applied recently [1]. Among them, Coherent Anti-Stokes Raman Scattering (CARS), a molecule specific laser spectroscopic diagnostic tool, is well developed to perform quantitative temperature and concentration measurements in practical combustion systems, and has been extensively used for several years. The diagnostic is usually performed by comparing experimental CARS spectra to a library of pre-calculated theoretical spectra, generated for different concentrations and temperatures. The application of this method requires fundamental studies such as broadening and shifting coefficients measurements because the signal intensities of the CARS lines strongly depend on the Raman line widths of the individual transitions. The latter are generally performed by Stimulated Raman Spectroscopy (SRS) in static cells, for reasons that will be explained later. Our attention was focused on H_2 because this molecule is present in abundance into the major part of the gas flowfield (except in the LOX core), and is thus used as a probe molecule. Water vapor being the only product of the cryogenic reaction $H_2 + \frac{1}{2}O_2 \rightarrow H_2O$, the H_2–H_2O system plays a key role in this application, but the influence of collisions with H_2O on the spectra of H_2 had not been studied before this work.

We will present the three steps of our work: in Sections 1 and 2, we will discuss the experimental determination of H_2 line parameters by Stimulated Raman Spectroscopy and the modelling of line parameters through simple polynomial laws. Section 3 will be devoted to the experimental determination of temperature on the Mascotte device at ONERA. Concluding remarks are then given in Section 4.

2. Experimental determination of line-parameters

2.1. The stimulated Raman effect

As explained in the introduction, the optical diagnostic in combustion media is usually achieved by comparing experimental CARS spectra to a set of theoretical spectra, calculated for different concentration and temperature conditions. This thus requires accurate knowledge of the line widths and line shifts of the Raman lines and their temperature dependence. With that aim, it is better to use another nonlinear Raman technique, the Stimulated Raman effect, instead of CARS to determine the line parameters in a static cell. Indeed, in CARS, the signal being proportional to the square of the third order nonlinear susceptibility $\chi^{(3)}$, the presence of a nonresonant background increases the complexity of the spectrum at high pressure, and makes difficult the extraction of line parameters. This does not occur with the Stimulated Raman technique for which the signal is proportional to the imaginary part of $\chi^{(3)}$. The profile of SRS lines is thus not distorted by the effects of interferences between the real and imaginary parts of the susceptibility. The extraction of the collisional linewidths is, thus, simplified.

SRS (Stimulated Raman Spectroscopy) is a third-order nonlinear process generated when two lasers with frequencies ω_1 and ω_2 are focused in a sample, without any phase matching conditions. When $\omega_1 - \omega_2$ equals the frequency of a transition of the studied species, a nonlinear polarization appears in the medium and induces the modification of the interacting waves. During the process, a gain is produced at frequency ω_2 (called the pump frequency), whereas photons with frequency ω_1 (probe frequency) are annihilated. The signal is detected either by measuring the gain at the frequency ω_2 (Raman Gain Spectroscopy) or the losses at the frequency ω_1 (Raman Loss Spectroscopy). In the second case, one also speaks of Inverse Raman Spectroscopy (IRS). Consequently, the probe laser which measures the interaction (i.e., the probe laser) must be very stable in intensity. Usually, cw ion lasers, such as Ar^+ or Kr^+ are chosen as a probe, whereas a pulsed laser is used as a pump.

2.2. The stimulated Raman spectrometer in Dijon

For our studies on H_2, the system in its inverse Raman configuration developed in Dijon is used [2]. The probe laser is a frequency-stabilized Ar^+-ion laser operating at 476.6 nm and providing approximately 300 mW in the cell. The tunable pump laser is a pulsed amplified cw ring dye laser operating at 594.3 nm using Rhodamine 6G dye. The peak power is usually limited to 100 kW so as to avoid possible Stark effects. The apparatus width induced by the pulse duration of 4–5 ns is about 90 MHz. The pump and the probe beams are crossed at a small angle in the gas sample with a 30-cm focal-length lens. Beams are then separated after the cell using a direct vision prism and optical filters and the probe beam which carries the Raman signal is directed on a fast photodiode (EGG FND 100), amplified in a 'boxcar' and stored in the data acquisition system.

2.3. Absolute frequency measurement

A homemade double Michelson wavemeter [3] provides accurate absolute measurements of the laser wavelenghts. The reference laser is a stabilized Helium–Neon laser (633 nm). The duration of a measurement is about 5 s. As the data acquisition count up to 10 million fringes with a precision of the order of the $1/100$ of fringe, the absolute frequency is known with a accuracy of approximately 3 MHz (10^{-4} cm^{-1}).

2.4. High pressure and high temperature Raman cell

In the past 10 years, efforts were focused on the development of a cell which could withstand high pressures (up to 5 MPa), high temperatures and the high chemical reactivity of water vapor simultaneously. This true technological challenge was taken up gradually, and the last prototype enabled us to performed measurements up to 1800 K in a H_2–H_2O mixture. The cell is made of Inconel® and the sapphire windows are placed close to the center so as to reduce the optical path of the beams in an area where density fluctuations can appear. The heating part consists of a platinum wire rolled around an alumina tube (7.5 cm length, 7.5 mm in diameter). The latter permits a good homogenization of the temperature and prevents the wire from subsiding. The whole is surrounded by an insulating material made of zirconium oxyde. A thermocouple (type 'B') placed along a generatrix of the tube controls the temperature. In order to prevent the condensation of water vapour, the whole external envelope of the cell, as well as the supports of the sapphire windows are preheated at 525 K by means of thermocoax wires.

All the measurements were performed in the collisional regime. The gas densities were calculated from the gas state equation using a virial correction limited to the second order. The virial coefficients were derived from experiments when available, or otherwise calculated according to [4]. However, the largest virial correction to the density was 1.5%.

2.5. Determination of line broadening coefficients of H_2 perturbed by H_2O

Careful attention has to be paid when measuring and analyzing H_2–X broadening coefficients. Indeed, it has been shown during the last decade that the H_2–X systems may have specific large inhomogeneous spectral features, due to the dependence of the line broadening and line shifting on the (H_2) radiator speed, particularly at high temperature [2,5–9]. The experimental spectral line shapes exhibit a marked asymmetry and a nonlinear behavior of the apparent broadening γ_{obs} as a function of concentration is observed. The consequence is that the contribution of the inhomogeneous broadening may be much larger than the collisional contribution, so that it is a priori necessary to account for these speed-dependent effects for an accurate application of CARS diagnostics.

These effects are now perfectly described, at any density regime, by speed-dependent line shape models developed at the Laboratoire de Physique Moléculaire, in Besançon (RTBT for the high density range [10], and HVCD + SVCD at any density [11]). Let us just mention that in a model such as RTBT, the speed-effects are governed by the fraction x^{RTBT} of collisions inducing speed classes exchange.

In the case of pure H_2, however, it has been shown, both experimentally (the observed profiles are symmetric and well fitted by a Lorentzian shape) and theoretically [12] that these effects strictly do not occur. This allows the direct determination of the broadening coefficients. Those have been measured for the $Q(J = 0{-}5)$ lines by Forsman et al. [13]. A linear behavior was observed as a function of the temperature. We have completed the measurements from 1000 K to 1800 K for the $Q(J = 0{-}7)$ lines [8]. The linear dependence as a function of the temperature is confirmed up to 1800 K and the coefficients are modeled as follows:

$$\gamma_{H_2-H_2}(T) = B_2 T + B_0.$$

A similar situation is encountered in the case of H_2–H_2O mixtures, since no distortion of the line shape (as can be seen on Fig. 1) was observed in this system. Moreover, the line broadening coefficients exhibit a linear dependence versus perturber concentration, within the experimental uncertainties. We concluded that the speed effects are obviously too weak to be

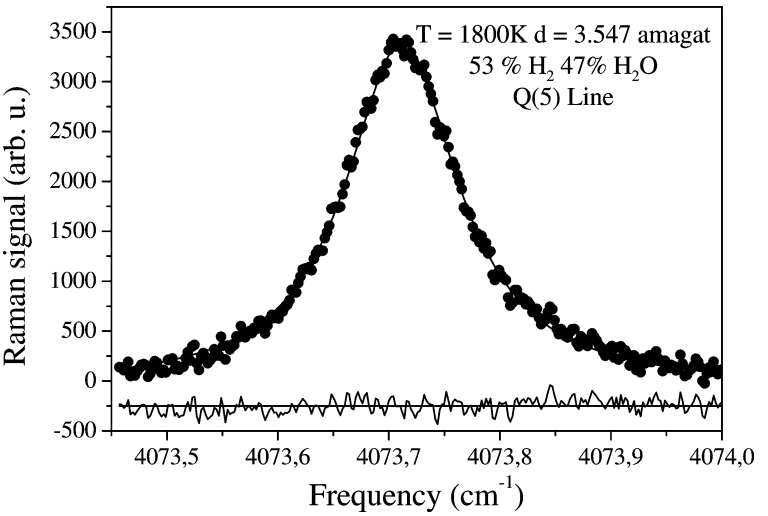

Fig. 1. Profile of the $Q(1)$ line of a binary mixture H_2–H_2O (53% H_2, 47% H_2O) at 1800 K and 3.5 amagat. The dots are experimental data points, the solid line is the best fit obtained with a Galatry profile. Below is the residual exp-calc.

observed, compared to the large collisionnal broadening, and it was then realistic to disregard them. The absence of apparent inhomogeneous signatures in the H_2–H_2O system has two consequences: the inhomogeneous broadening cannot be extracted from the experimental profile (at least for binary mixtures), and the line shape analysis can be performed by using the usual Lorentzian profile, or equivalently by setting x^{RTBT} equal to 1 in the RTBT model. Those hypothesis allowed one to first modelize these coefficients by means of a simple polynomial law which permits temperature extrapolations with a narrow confidence band.

In that case, the apparent broadening and the homogeneous collisional broadening are thus supposed to be the identical. In other words, the apparent broadening coefficient Γ^0 expressed per density units is supposed to follow the usual linear mixing rule:

$$\Gamma^0 = C_{H_2}\Gamma^0_{\mathrm{H_2-H_2}} + C_{\mathrm{H_2O}}\Gamma^0_{\mathrm{H_2-H_2O}}, \tag{1}$$

where $\Gamma^0_{\mathrm{H_2-H_2O}}$ does not depend on the concentration, and a simple Lorentzian profile has been used to analyze the spectra.

All the measurements have been performed at 4 or 5 amagats, in density conditions above the Dicke minimum [14] (about one amagat for the $Q(1)$ line). Consequently, the apparent linewidth Γ at a given density ρ and temperature T is

$$\Gamma(\rho, T) = \Gamma^{\mathrm{Obs}}(\rho, T) - \frac{2\pi D(T)\omega^2}{c\rho}, \tag{2}$$

where the last term accounts for the Doppler residual. $\Gamma(\rho, T)$, $\Gamma^{\mathrm{obs}}(\rho, T)$ and ω the Raman frequency of the studied transition at zero density are expressed in cm^{-1}, $D(T)$ is the diffusion constant expressed in cm^{-2} amagat^{-1}, and c the speed of light. The apparent broadening coefficient is then defined as $\Gamma^0 = \Gamma(\rho, T)/\rho$.

In our previous studies below 1000 K on H_2–H_2O mixtures, a slight nonlinearity has been observed for some Q-branch lines, as well as on pure rotational lines $S_0(J)$. Michaux [8] proposed to add a square-root temperature term in the linear law, so as to account for the curvature at lower temperature, while keeping the asymptotic linear behavior. The inclusion of the nonlinearity permits a slightly better description of the observed data. The new measurements performed at 1500 and 1800 K have confirmed the need to use such a nonlinear law:

$$\Gamma^0_{\mathrm{H_2-H_2O}}(T) = \Gamma_2 T + \Gamma_1\sqrt{T} + \Gamma_0. \tag{3}$$

The straight forward consequence of this simple polynomial law is the possibility to easily perform extrapolations to flame temperatures. In Fig. 2 we plotted the experimental data as well as the fit using Eq. (3). The confidence band at 95% connected to the extrapolation up to 3000 K by means of Eq. (3) is also shown on Fig. 3 for the $Q(5)$ line. One understands the importance of the new data at 1500 and 1800 K that have significantly reduced the uncertainty range tied to the extrapolations. Similar results have been obtained for the other measured $Q(J)$ lines.

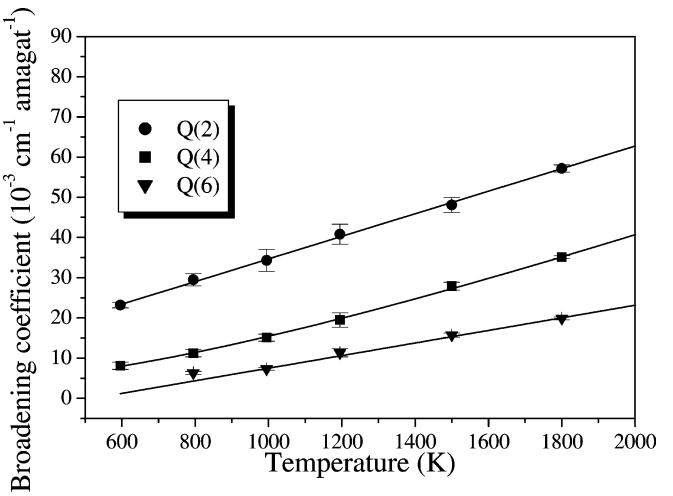

Fig. 2. $Q(J)$ experimental broadening coefficients of H_2 infinitely diluted in H_2O in mK/amagat versus temperature T (K). The solid line shows the fit to the nonlinear law $\Gamma^0_{H_2-H_2O}(T) = \Gamma_2 T + \Gamma_1\sqrt{T} + \Gamma_0$.

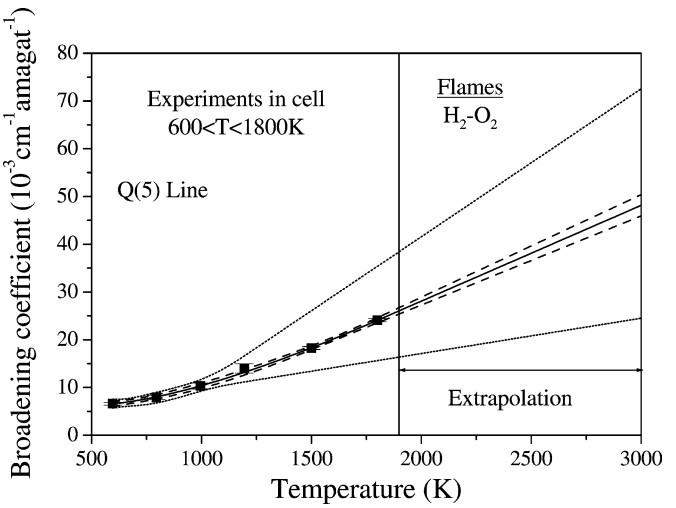

Fig. 3. 95% confidence band relative to the extrapolations of the broadening coefficients of of H_2 infinitely diluted in H_2O for the $Q(5)$ line to flame temperature. In dots, the confidence band for the extrapolation using data up to 1200 K, in dashed lines, the confidence band for the extrapolation using data up to 1800 K.

3. Diagnostics on MASCOTTE facility

3.1. Fundamentals of CARS

Coherent anti-Stokes Raman scattering (CARS) has received considerable attention over the last two decades for combustion diagnosis based upon the pioneering investigations of Taran and co-workers [15]. Excellent review papers are given in [16–18]. CARS is an example of a four wave parametric process in which three waves, two at the pump frequency (ω_P) and one at the Stokes frequency (ω_S) are focused to the measurement point in the sample to produce a new coherent beam at the anti-Stokes frequency ($\omega_{AS} = 2\omega_P - \omega_S$). The strength of the interaction depends on the third-order susceptibility of the medium, which is greatly enhanced when the frequency difference ($\omega_P - \omega_S$) matches a Raman active vibrational resonance in the medium. The nonlinear susceptibility is density and temperature-dependent providing the basis of diagnostics. Temperature measurements may be derived from the spectral shape of the signal obtained by scanning the frequency of a narrow bandwidth Stokes laser or, when probing a turbulent flow by use of a broad bandwidth Stokes laser which allows the capture of a multiplexed spectrum from a single laser shot.

3.2. CARS experimental setup

The laser system is composed of two separate optical benches which produce the pump and Stokes beams required for H_2 spectroscopy. The pump beam is the doubled-frequency output of a Nd:YAG laser chain composed of a single-mode Q-switched oscillator followed by an amplifier. The laser delivers pulses with a frequency rate of 10 Hz, providing single-shot measurements that can be used to study the dependence/variability of a process. Half of the green energy is used to pump the Stokes dye laser which emits the broadband ω_2 beam centered at 683 nm with a 200 cm^{-1} bandwidth (FWHM). At the output of the laser bench, the pump beam is split in two parallel beams and one of them is overlapped with the ω_2 beam (planar BOXCARS geometry) [16].

The laser beams are focused first in a atmospheric pressure flux flow of argon where a nonresonant CARS signal is created to monitor the shot to shot fluctuations of pulse energy of the lasers beams and of the spectral shape of the Stokes laser. The focal volume is positioned axially and radially in the combustion chamber by moving the optical lenses by means of translational stages.

Reference and sample CARS spectra are dispersed using two separate spectrometers. The CARS spectrum and the broadband reference are formed in the output plane of the spectrographs and detected by means of intensified 512-photodiode arrays (OMA III 1420B/512/HQ-FP).

3.3. The MASCOTTE facility

The combustion chamber is equipped with a single-element injector fed by LOX and GH_2. The geometry of the injector element consists of a central tube of 5 mm inner diameter fed with LOX surrounded by a parallel annular duct of 12 mm diameter fed with gaseous hydrogen. Liquid oxygen is injected at a temperature of 85 K, while gaseous hydrogen is injected at room temperature. The combustion facility is a square duct of 50 mm inner dimension (Fig. 4) where four fused silica windows allow an optical access. The two lateral ones are 100 mm long and 50 mm high. The upper and lower windows are 100 mm long and 10 mm in width. The combustion chamber is mounted horizontally and its centerline is the x-axis with zero located as the exit of the injector. The y- and z-axes are diametrical to the combustor cross-section with the y-axis aligned with the laser beams.

3.4. The temperature determination at high pressure

In the case of high density media (i.e., pressure above 0.1 MPa), two phenomena become important. The first is pressure broadening which is caused by collisional processes and the second is related to the Dicke narrowing [14]. This last effect is a result of a coupling of the Doppler effect to the collisional one as collision frequency increases. It results from a coherent averaging of frequencies within the normal Doppler line profile, induced by velocity-changing collisions that conserve vibrational phase. If the frequency of velocity-changing collisions is greater than that of dephasing collisions, line narrowing

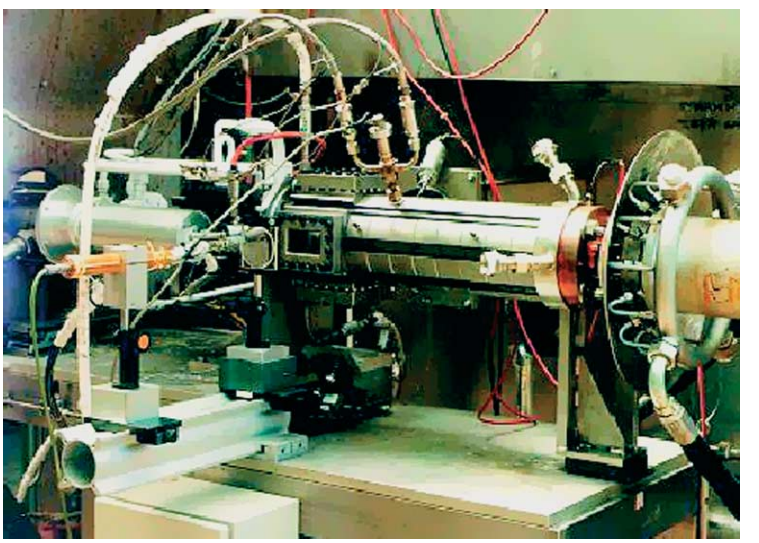

Fig. 4. The MASCOTTE combustion facility.

is observed. This phenomenon is represented by a soft collision model such as the well-known Galatry model [19] which has been suitably used for many collisional systems. The complex Galatry function describes the observed spectra whatever the density. This property is important in CARS thermometry because the temperature being unknown, the density is unknown in the considered probed gas volume. The pressure shift of lines has been omitted since it produces merely a small overall shift of the Q-branch spectrum. The important parameter is then the collisional broadening. This coefficient depends on the density, the J quantum number, the temperature and the composition of the mixture as shown above.

A specific analytical procedure was developed and employed to reduce CARS spectra to temperatures despite the lack of knowledge of species composition. For each pressure condition, a library of theoretical CARS spectra was created at 50 K

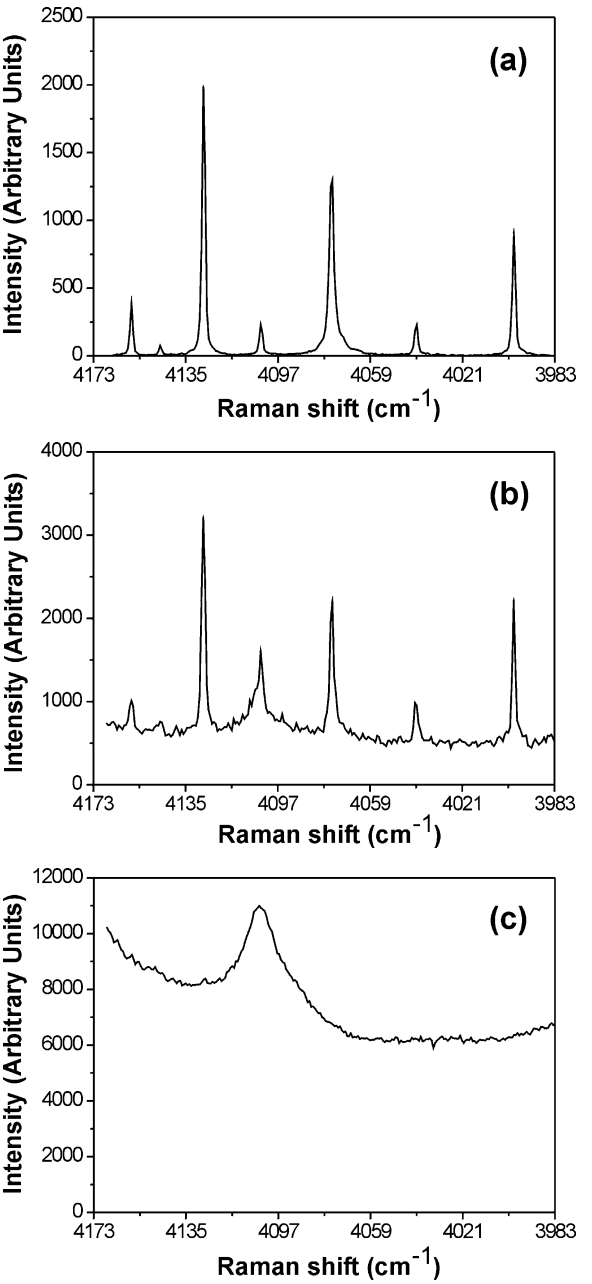

Fig. 5. Experimental H_2 CARS spectra recorded with different breakdown levels: (a) no breakdown case; (b) intermediate case; (c) breakdown case.

increments over the range 300–3000 K and at 5% increments for the H_2 and H_2O molar fractions. The experimental spectra were compared to the theoretical library spectra with a simple least-squares fitting procedure to get temperatures. The error function is then defined by

$$F = \sum \omega_j \left[I_j^{\text{exp}} - I_j^{\text{theo}}(T, C_{H_2}, C_{H_2O}) \right]^2, \tag{4}$$

where ω_j is a statistical weight characteristic of the lines magnitude. C_{H_2} and C_{H_2O} are the molar fractions of H_2 and H_2O using the assumption, $C_{H_2} = 1 - C_{H_2O}$.

3.5. Data analysis

Depending on the locations in the flame, the CARS spectra present some distortion in shape and in intensity which can complicate the interpretation of CARS spectra. Fig. 5 illustrates these variations by comparing a H_2 CARS spectrum without distortion to CARS spectra with different levels of perturbations. Experimental observation indicates that the variation could be related to the presence of a background signal which may swamp the CARS signal (Figs. 5(b), (c)). Studies of the origin of this background suggest that it is caused by laser-induced breakdown generated in the liquid phase. The resulting plasma is

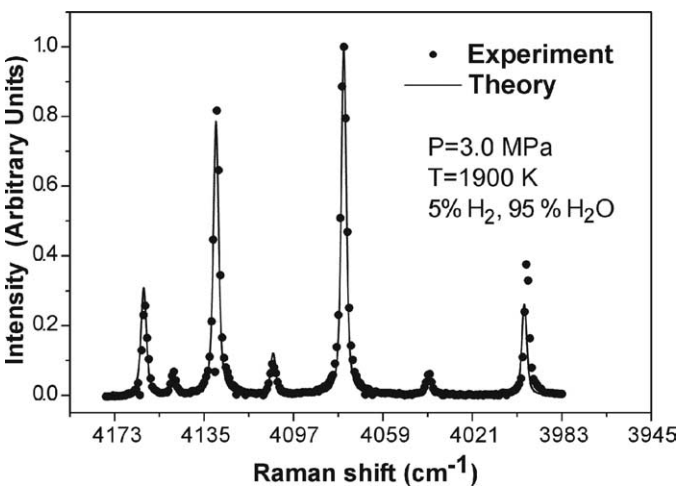

Fig. 6. Comparison of experimental H_2 CARS spectrum to calculated spectrum at 3.0 MPa. The best fit theoretical spectrum corresponds to a temperature of 1900 K and molar fractions of H_2 and H_2O, $C_{H_2} = 0.05$ and $C_{H_2O} = 0.95$.

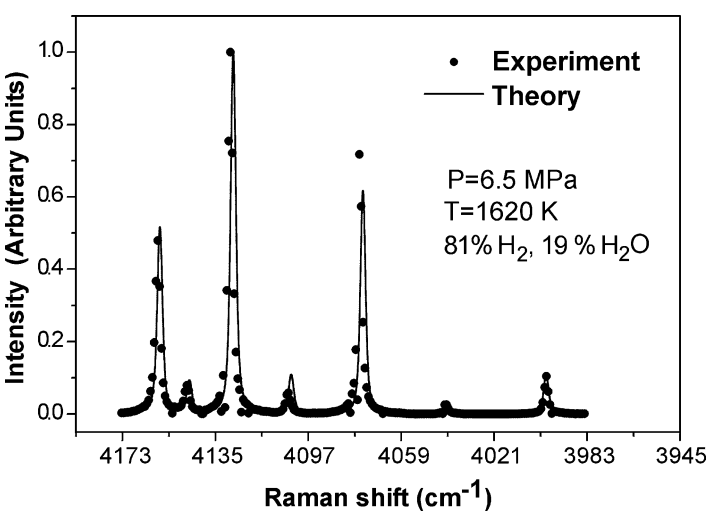

Fig. 7. Comparison of experimental H_2 CARS spectrum to calculated spectrum at 6.5 MPa. The best fit theoretical spectrum corresponds to a temperature of 1620 K and molar fractions of H_2 and H_2O, $C_{H_2} = 0.81$ and $C_{H_2O} = 0.19$.

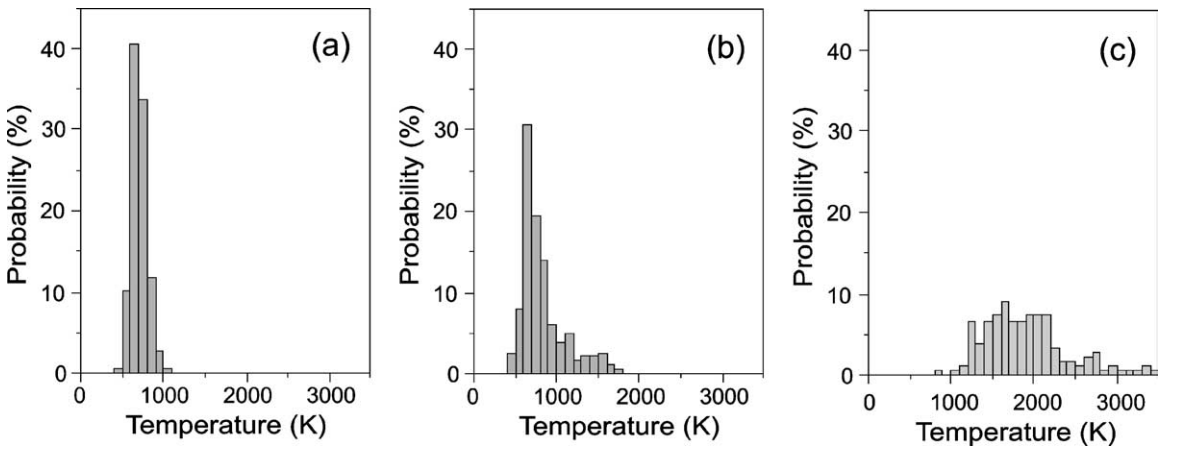

Fig. 8. CARS Temperature probability density distributions from single-shot spectra obtained at a radial position of $y = 20$ mm and at different axial positions: (a) $x = 15$ mm; (b) $x = 50$ mm; (c) $x = 150$ mm. Operating condition: $p = 6.5$ Mpa.

then composed of ions and atoms that have large third-order nonresonant susceptibilities, producing then a nonresonant CARS signal large enough to compete with the hydrogen one. This trend is clearly illustrated in Fig. 5(c) where the spectral signature corresponds to laser-induced breakdown emitted by the neutral O transition located at 436.8 nm. The extent of this effect is related to the intensity and spatial quality of the laser beams, the droplets loading and the molecular number density of the medium. This problem is partially circumvented by reducing the beam intensities to the breakdown threshold of the medium allowing then the generation of reliable CARS spectra.

In the case where no perturbation affect the CARS spectra, it is then possible to deduce temperature from single-shot CARS spectra. Figs. 6 and 7 display typical single-shot CARS spectra obtained in the Mascotte facility at pressures of 3.0 and 6.5 MPa along with the best theoretical results deduced from the spectra fitting procedure. As this procedure compares the square root of intensity in the least-squares fitting process, all subsequent results will be plotted as such. Both spectra display excellent agreement between data and theory. Not only are the peak intensities of each transition generally closely matched by the theory, but the linewidth and lineshape are as well. Detailed small discrepancies between the theoretical and experimental spectra probably arise from laser power fluctuations not totally corrected in the present conditions and from possible uncertainties related to the lacking in precision of the linewidth parameters at high temperature, i.e., above 1900 K where no linewidth measurements in the high-pressure Raman cell were performed.

To evaluate the effects of uncertainty in the collisional linewidths on the accuracy of temperatures, CARS spectra were calculated with a 10% variation of the collisional linewidths. Whatever the range encompassing the expected flame temperature, the resulting maximum error on the inferred temperature never exceeds 50 K. Adding all the possible sources of errors (amplitude fluctuations that arise from the response characteristics of the optical detection, measurement uncertainties on peak amplitude related to the Poisson uncertainty, random dye laser intensity distribution, spectral distortions and disruption of the CARS signals, and beam steering and defocusing due to density gradients) provides an uncertainty on temperature of about 6–8%.

Analyzing the complete set of data also provided an insight of the flame structure at high pressure. For instance, Fig. 8 presents typical histograms of temperatures performed from series of 300 instantaneous measurements acquired at different locations downstream of the nozzle at 6.5 MPa. These results provide temperature histograms from the recirculation zone to the reacting shear layer. At $x = 15$ mm, a narrow and symmetric temperature distribution with a mean temperature of 700 K is observed indicating that hot gases formed downstream recirculate in this region (Fig. 8(a)). The bimodal nature of the histogram confirms the presence of large-scale coherent structures within the reacting shear layer (Fig. 8(b)). These structures form as folds around the flame edge, and then grow in size downstream, entraining reactants and products and thickening the reacting shear layer as shown on Fig. 8(c).

4. Conclusion

For several years, Coherent anti-Stokes Raman Spectroscopy (CARS) has been successfully demonstrated and extensively used for thermometry, pressure and concentration measurements in combustion environments, owing to its appropriate temporal and spatial resolutions. In the aim to improve the accuracy of temperature measurements in cryogenic rocket engines using the H_2–O_2 system, studies of H_2O-broadened H_2 lines by means of high-resolution stimulated Raman spectroscopy (SRS) have

been performed for the first time up to 1800 K thanks to the construction of a new cell which can support water vapour chemical reactivity. Because of its presence in nearly all regions of the combustion chamber, H_2 is indeed the natural probe molecule. Particular caution is a priori necessary for this application, since H_2–X systems exhibit speed inhomogeneous spectral features, such as a nonlinear dependence of the observed broadening as a function of concentration. But in the case of H_2–H_2O, neither experimental evidence of asymmetry nor nonlinearity of the broadening coefficient had been observed so far, which allows a direct determination of the collisional broadening parameter, without using specific speed-dependent models. The useful parameters have been modeled by means of simple polynomial laws, in order to predict the line broadening to flame temperatures (3000 K) with a narrow confidence band.

The application of CARS for temperature measurements in high pressure cryogenic GH_2/LOX combustors was also successfully demonstrated. Single-shot measurements were performed in the MASCOTTE test facility with a spatial resolution in beam direction of $\sim$1 mm. The estimated accuracy of single-shot temperatures for H_2 is 6–8%. Experiment reveals that droplet laser-induced breakdown can cause serious problems in making temperature measurements using CARS into the core flow where LOX is mainly present. Rejecting spectra with a low signal-to-noise ratio in the data reduction provides reasonable CARS temperature measurements which can be used to characterize the performance of the combustors, in particular the fuel/LOX mixing and the combustion efficiency.

Acknowledgements

This work was financially supported by SNECMA-Division Moteurs fusées and by the French space agency (CNES). Support by L. Vingert, J. Champy and A. Mouthon from Onera, who provided technical assistance, is also gratefully appreciated.

References

[1] S. Candel, G. Herding, R. Snyder, P. Scouflaire, C. Rolon, L. Vingert, M. Habiballah, F. Grisch, M. Péalat, P. Bouchardy, D. Stepowsky, A. Cessou, P. Colin, Experimental investigation of shear coaxial cryogenic jet flames, J. Propulsion and Power 14 (1998) 826–834.
[2] J.Ph. Berger, R. Saint-Loup, H. Berger, J. Bonamy, D. Robert, Measurement of vibrational line profiles in H_2-rare gas mixtures: determination of the speed dependence of the line shift, Phys. Rev. A 49 (1994) 3396.
[3] R. Chaux, C. Millan, G. Millot, B. Lavorel, R. Saint-Loup, J. Moret-Bailly, Mesures de longueurs d'onde de lasers continus à l'aide d'un lambdamètre. Application à l'étalonnage de spectres Raman à haute résolution, J. Optics (Paris) 19 (1) (1988) 3.
[4] J.O. Hischfelder, C.F. Curtiss, R.B. Bird, Molecular Theory of Gases and Liquids, Wiley, New York, 1964.
[5] R.L. Farrow, L.A. Rahn, G.O. Sitz, G.J. Rosasco, Observation of a speed-dependent collisional inhomogeneity in H_2 vibrational line profiles, Phys. Rev. Lett. 63 (1989) 746.
[6] J.Ph. Berger, Mécanismes de relaxation collisionnelle dans l'hydrogène et l'azote en mélange gazeux. Application à la thermométrie optique dans les moteurs cryogéniques et les moteurs à combustion interne, Thesis, Université de Bourgogne, France, 1994.
[7] P.M. Sinclair, J.Ph. Berger, X. Michaut, R. Saint-Loup, R. Chaux, H. Berger, J. Bonamy, D. Robert, Collisional broadening and shifting parameters of the Raman Q branch of H_2 perturbed by N_2 determined from speed-dependent line profiles at high temperatures, Phys. Rev. A 54 (1996) 402.
[8] X. Michaut, Influence de la relaxation collisionnelle sur les raies Raman purement rotationnelles de H_2 perturbé par H_2, He, Ar, N_2 et H_2O en vue du diagnostic optique de la température. Comparaison avec les raies rovibrationnelles de la branche Q, Thesis, Université de Bourgogne, France, 1999.
[9] F. Chaussard, Etude expérimentale et théorique des mécanismes collisionnels à haute densité. Application au diagnostic de la température dans un moteur croygénique, Thesis, Université de Bourgogne, France, 2001.
[10] D. Robert, J.M. Thuet, J. Bonamy, S. Temkin, Effect of speed-changing collisions on spectral line shape, Phys. Rev. A 47 (1993) 771.
[11] B. Lance, D. Robert, An analytical model for collisional effects on spectral line shape from the Doppler to the collision regime, J. Chem. Phys. 109 (1998) 8283;
B. Lance, D. Robert, Correlation effect in spectral line shape from the Doppler to the collision regime, J. Chem. Phys. 111 (1999) 789.
[12] P.N.M. Hoang, P. Joubert, D. Robert, Speed dependent line shape models analysis from molecular dynamics simulations. I – the collision regime, Phys. Rev. A 65 (2001) 0125.
[13] J.W. Forsman, J. Bonamy, D. Robert, J.Ph. Berger, R. Saint-Loup, H. Berger, H_2–He vibrational line shape parameters: measurements and semi-classical calculations, Phys. Rev. A 52 (1995) 2635.
[14] R.H. Dicke, The effect of collisions upon the Doppler width of spectral lines, Phys. Rev. 89 (1953) 472.
[15] P.R. Regnier, J.P. Taran, On the possibility of measuring gas concentrations by stimulated anti Stokes scattering, Appl. Phys. Lett. 23 (1973) 240–242.
[16] S. Druet, J.P. Taran, CARS spectroscopy, Prog. Quant. Electr. 7 (1981) 1–72.
[17] A.C. Eckbreth, Laser Diagnostics for Combustion Temperature and Species, second ed., Gordon and Breach, 1996.
[18] D.A. Greenhalgh, Quantitative CARS spectroscopy, in: R.J.H. Clark, R.E. Hester (Eds.), Advances in Non-Linear Spectroscopy, vol. 15, Wiley, 1988.
[19] L. Galatry, Simultaneous effect of Doppler and Foreign gas broadening on spectra lines, Phys. Rev. 122 (1961) 1218–1223.